EVALUATION OF DNB INDUCED FATIGUE IN HEAT TRANSFER TUBES

S. A. KAMAL, D. H. PAI, J. M. CHERN

Advanced Engineering Methods, Engineering Technology Department, Foster Wheeler Energy Corporation, 110 South Orange Avenue, Livingston, New Jersey 07039, U.S.A.

Abstract

In the DNB (Departure from Nucleate Boiling) region of steam generator evaporator, the heat transfer tubes are subjected to oscillating thermal condition with high frequency and the resulting high cycle fatigue damage in these tubes is usually evaluated on the basis of the alternating stress intensity and the mean stress intensity during the thermal cycle. Due to the three-dimensional nature of thermal loading, a three-dimensional stress analysis is required to rigorously determine the stress intensity. However, in practical design, simplified stress analyses with proven validity are preferred because of the analytical complexity involved in the three-dimensional analysis. This paper presents a systematic numerical comparison of the simplified and three-dimensional analyses and recommends an appropriate simplified model for practical applications.

A three-dimensional stress analysis was first performed using a general purpose finite element program and a three-dimensional temperature history which is generated by a new thermal model consisting of revolving rivulets. The thermal loads for the simplifide models were derived from this general temperature field. The fatigue life was assumed to depend on the maximum equivalent alternating stress intensity which was evaluated based on the Goodman diagram. The simplified structural models analyzed include: 1) generalized plane strain 2-D (r,θ) model with temperature and stress variations in the radial and circumferential directions; 2) axisymmetric 2-D (r,z) model with radial and axial variations; and 3) generalized plane strain 1-D (r) model with only radial variation.

Among the simplified models, the 2-D (r,θ) model gives the best results, which are practically the same as that of the 3-D model. Such an excellent agreement is due to the approximate generalized plane strain condition in the critical axial region of the 3-D model where the temperature fluctuation and alternating stress attain their peak values. The calculation cost of the simplified model, however, was two order of magnitude less than the 3-D model when the same general purpose finite element program is used. The use of special purpose computer program in the simplified analysis further reduced the calculation cost. It was also revealed that the results were practically unchanged when the thermal loading generated with a consistent 2-D (r,θ) model was used.

It is therefore recommended that a combined 2-D (r,θ) thermal and stress model be used in evaluating the alternating stress intensity in the DNB region.

1. Introduction

In the DNB (Departure from Nucleate Boiling) region of steam generator evaporator, the heat transfer tubes are subjected to oscillating thermal condition with high frequency and the resulting stress condition of alternating nature may lead to severe fatigue damage of the tubes and deserves special design consideration. The evaluation of this type of fatigue problem usually consists of two analyses: a thermal analysis in which the temperature field is determined, followed by a stress analysis in which the stress histories are first determined, then analyzed to obtain some parameters (such as alternating stress intensity and mean stress), and finally, the fatigue curves are used to make fatigue damage prediction. Due to analytical complexity as well as lack of experimental data for confirmation, rigorous three-dimensional analyses are rarely performed. Instead, simplified approaches in both thermal and stress analyses are adopted in design practice.

Intensive efforts have been made recently to understand the fatigue damage in the DNB region. The various simplifications made in these investigations can be briefly summarized as follows: a) a wave front model in which a wave form of heat transfer coefficient with a longitudinal variation is assumed to move back and forth along the tube and the resulting axisymmetric thermal stress analysis is treated as a one-dimensional (r) or a two-dimensional (r,z) problem [1,2]; b) an axisymmetric one-dimensional (r) thermal stress model in which the time variation of temperature matches the measured temperature fluctuation at the thermocouple location [3]; c) the two-dimensional (r,θ) hopping rivulet model in which rivulets with certain circumferential distribution stay at the same locations of the tube circumference for half of the temperature cycle, then instantaneously disappear at the time when rivulets of the same distribution appear at new locations, and the new rivulets stay at these new locations for the second half of the temperature cycle [4,5].

In view of the various simplifications made in the above-mentioned investigations, it is desirable to make a systematic comparison of simplified analyses so that a simplified structural model can be selected for use in practical design analysis. For this purpose, the present investigation utilizes a thermal model in which the oscillation of temperature cycle is simulated with continuously revolving rivulets [6]. Such a thermal model is more flexible than the hopping rivulet model in generating the fluctuating temperature field in that no points of the tube inside surface are constantly wet or dry during the entire thermal cycle (except at the two ends of the DNB zone). For the present purpose of stress evaluation, it suffices to note that such a thermal model can be used to generate three-dimensional temperature field as well as approximate temperature distributions which are two- or one-dimensional in spacious variation, and also that the models with three and four rivulets have the best agreement with test results. Justifications and details of this thermal model are given in reference [6].

A three-dimensional (r,θ,z) stress analysis is first performed and the results form the basis of comparison for the other simplified models including those with (r,θ), (r,z), and (r) spatial variations, where (r,θ,z) are the conventional cylindrical coordinates. The thermal loads used in these simplified models are either derived from the three-dimensional thermal results or obtained with corresponding simplified thermal models.

2. Basis of Fatigue Life Evaluation

A variety of parameters have been used in experimental correlations of fatigue life

[7]. The most dominant parameter that has been commonly used in design analysis of metal structures is the ductility (strain range) of the structures under cyclic loadings. Due to the large number of thermal stress cycles in the tube wall under DNB conditions (in the order of 10^8 cycles during the lifetime), the fatigue life under consideration is of the high cycle type. Therefore, the nominal stress-strain is most likely in the elastic regime and the strain range used in the fatigue evaluation may be replaced by the stress range. Even when plastic strains of moderate magnitude are present, the stress range may still be used in the fatigue life evaluation if the tube shakes down to an elastic state after a limited number of thermal cycles. Unlike the low cycle fatigue wherein the plastic strain of substantial magnitude may render the stress oscillating approximately between the tensile and compressive yield stresses and thus resulting in mean stress of small magnitude, the effect of mean stress on high cycle fatigue may be significant. Therefore, the fatigue life (number of load cycles to failure) in the present investigation is assumed to be a function of equivalent alternating stress intensity (S_{eq}) which is determined by adjusting the alternating stress intensity (S_{alt}) to account for the mean stress (S_{mean}) effect according to the Goodman diagram:

$$S_{eq} = S_{alt} / (1 - S_{mean}/S_u)$$

S_u being the ultimate tensile strength of the tube material. From the stress analysis result, the stress intensity (shear stress) history at each material point has to be calculated and the values of S_{alt} and S_{mean} that maximize S_{eq} be chosen. Since the shear stress history in a general situation depends on the orientation, the maximum possible value of S_{eq} must be selected from those values at different orientations.

Standard procedures [8] have been available for calculating the maximum value of S_{alt} (i.e., S_{eq} without the effect of S_{mean}). In these procedures, the cases of constant and varying principal stress directions are considered separately. In the case of constant principal stress direction, the time-history of stress intensity (shear stress) can be defined for specific directions which are fixed in time and represent the orientations of maximum shear stress; the S_{alt} values can therefore be determined accordingly. The standard procedure for this special case can be extended to include the effect of S_{mean} since this value can be determined from the well-defined shear stress history.

The case of varying principal stress direction is more involved since the orientations of maximum shear stress vary in time and the shear stress history has to be considered in various fixed orientations. In this case, the standard procedure of reference [8] applies only if the effect of S_{mean} is neglected. To account for the effect of S_{mean}, different orientations have to be considered and the calculations, although straightforward, become more tedious [7].

3. Three-Dimensional (r,θ,z) Analysis

A three-dimensional stress analysis was performed with finite element program [9]. The model was constructed using the three-dimensional isoparametric solid elements in their general form, i.e., with six stress/strain components. The cross-sectional tube dimensions of 15.75 mm O.D. x 2.90 mm thickness and the length of the transition boiling region of 38.10 mm were selected [3]. The material properties used in this stress analysis and all the simplified analyses corresond to the 2¼ Cr-1 Mo steel.

The effort of the analysis can be greatly reduced by taking advantage of the periodic nature of the problem and utilizing the superposition principle. Since the rivulet pattern is revolving at a constant rate along the circumference, the temperature distribution as well as the structural response at any time are periodic in θ with a period of $\alpha = 2\pi/n$, n being the number of rivulets. Furthermore, if the reference solution $S_o(r,\theta,z,t_o)$ at a reference time, say t_o, is determined for a sector $0 \leq \theta \leq \alpha$, then the response $S(r,\theta,z,t)$ at any time t can be taken as $S_o(r,\theta - \beta,z,t_o)$, where $\beta = \alpha(t-t_o)/\tau$, τ being the period of temperature versus time fluctuation.

The three-rivulet finite element mesh consisted of 2,100 elements and 2,880 nodal points. The nodes were equally spaced in the radial (5 nodes), circumferential (16 nodes) and axial (36 nodes) directions. The four-rivulet finite element mesh was similar to the three-rivulet mesh, except the sector size was reduced from 120 degrees to 90 degrees. The numbers of nodal points in the radial and circumferential directions were kept the same at 5 and 16, respectively. The number of the nodal points in the axial direction was increased from 36 to 41. Thus, the total mesh consisted of 2,400 elements and 3,280 nodal points.

The temperature distribution $T(r,\theta,z,t_o)$ obtained from the thermal analysis of the three-dimensional rivulet model provided the nodal point temperatures for the finite element model. The reference time t_o was selected sufficiently long to ensure steady-state thermal solution. In addition to the cyclic thermal loads, a steam pressure of 11.4 MPa was applied to the tube inner surface.

The axial variations of the maximum fluctuation of the through-the-wall temperature difference, $\Delta\Delta T$, are shown in Figure 1. The $\Delta\Delta T$ is defined as

$$\Delta\Delta T = \max(T_o - T_i)_t - \min(T_o - T_i)_t$$

where $(T_o - T_i)_t$ is the time-history of the temperature difference through the tube wall. The resulting alternating stress intensity S_{alt} is shown in Figure 2. When the mean stress effect is included, the equivalent alternating stress intensity is obtained as shown in Figure 3. These values of S_{alt} and S_{eq} are at the inner surface of the tubes where the maximum temperature and stress fluctuations occur.

Since the wetness is assumed to vary linearly in the DNB zone from 0 at one end to 100% at the other end [6], the axial variations of $\Delta\Delta T$, S_{alt} and S_{eq} may be considered as the variations with respect to the percentage of wetness. One can easily see in Figures (1) to (3) that between 30% and 40% wetness, the variables $\Delta\Delta T$, S_{alt} and S_{eq} reach and almost maintain their maximum values in both models. Therefore, in the 3-D analysis, the maximum S_{alt} and maximum S_{eq} occur in a zone characterized by a very small temperature gradient in the axial direction. The importance of this phenomenon will be illustrated later when the simplified models are considered. The circumferential variations of the stress results at the axial location where $\Delta\Delta T$ is maximum, indicated a large difference in the fluctuation magnitude of the stress components in the circumferential and axial directions. For example, in the 3-rivulet model, the hoop stress component has an amplitude of 17.4 MPa while the axial component amplitude equals 119.5 MPa which is about seven times the hoop value. The same phenomenon is also observed in the 4-rivulet model results.

A useful correlation can be established by considering the maximum $\Delta\Delta T$ as a measure of the cyclic thermal load. It follows that according to the 3-D model results:

$$\left.\begin{aligned} S_{alt}/\Delta\Delta T &= 1.42\ MPa/^{o}C \\ S_{eq}/\Delta\Delta T &= 1.89\ MPa/^{o}C \end{aligned}\right\} \text{ for 3-rivulet model}$$

$$\left.\begin{aligned} S_{alt}/\Delta\Delta T &= 1.35\ MPa/^{o}C \\ S_{eq}/\Delta\Delta T &= 1.81\ MPa/^{o}C \end{aligned}\right\} \text{ for 4-rivulet model}$$

Therefore, for the same $\Delta\Delta T$, the 3-rivulet model gives slightly higher (4.5%) alternating stress than the 4-rivulet model does.

4. Simplified Stress Analyses

4.1 Generalized Plane Strain 2-D (r,θ) Model

Simplified stress analysis using this model were performed with finite element program [9] and simplified computer code [10], both of which gave similar results. The thermal loads adopted in the analysis were either extracted from the 3-D (r,θ,z) thermal results corresponding to a critical axial location z_{cr} or generated with a 2-D (r,θ) thermal model.

In the first loading case, the S_{eq} values obtained by the simplified analyses were found to differ from the 3-D result at z_{cr} by only 1%. Such excellent agreement is attributed to the approximate generalized plane strain condition near z_{cr} where the temperature fluctuation and the induced alternating stresses show very small axial variations.

Similar good results are also obtained in the second thermal loading simulation. Indeed, it was found that the $(S_{eq}/\Delta\Delta T)$ values obtained by the simplified model differ from the 3-D results by no more than 1%, while the difference in $\Delta\Delta T$ between the 2-D and 3-D models was about 2%.

4.2 Axisymmetric 2-D (r,z) Model

The axisymmetric thermal load for this model was extracted from the 3-D temperature distribution corresponding to a fixed circumferential location. Analyses were performed with finite element program [9] and special purpose code [11], both of which gave similar results. Based on the comparison of the axial variations of stresses with three rivulets, it was found that the 2-D model has a peak S_{alt} value of 53.6 MPa at 21% wetness while the 3-D model has a value of 59.7 MPa at 31.0% wetness, the difference in S_{alt} being about 10%. Because of the higher S_{mean} value predicted by the simplified model, the difference in S_{eq} was only about 2%. However, it was also observed that the stress fluctuation during the load cycle was dominated in magnitude by the axial component in the 3-D model, while the hoop and axial components are of almost identical magnitude in the 2-D model.

4.3 Axisymmetric 1-D (r) Model

The thermal load for this model was obtained from the temperature distribution of the 2-D (r,z) taken at a critical axial location corresponding to 31.0% wetness where the $\Delta\Delta T$ reaches its maximum value. Analyses were performed again with finite element program [9] and special purpose code [12], and similar results were obtained. The S_{alt} value obtained with this simplified model is 4% smaller than that of the 2-D (r,z) model and 17% smaller than the 3-D result. Also, because of the axisymmetric condition imposed, the hoop stress fluctuation in this simplified model is distinctively different from that of the 3-D model. However, this simplified model does have the advantage of simplicity, especially when the thermal load can be determined with a similar model.

5. Conclusions

The elastic analysis results of the various structural models, along with the associated CPU times using a CDC 7600 computer, are summarized in Table 1. Among the various simplified models considered, the 2-D (r,θ) model has the best agreement with the 3-D (r,θ,z) model in both stress intensities and overall stress pattern, and is therefore recommended for design/analysis use. The other simplified models also give reasonable, although less accurate and slightly nonconservative results for the stress intensity. However, it should be noted that since the fatigue damage is very sensitive to stress intensity, a slight difference in stress intensity prediction may be substantially magnified when it is translated to fatigue damage.

As for the computational cost, substantial saving can be gained with the use of simplified models. For instance, when finite element code is used, the CPU time for the 2-D (r,θ) model is about two-order of magnitude less than that for the 3-D model. The use of special purpose codes in the simplified analyses can further reduce the calculational cost.

The thermal load in the simplified analyses can be extracted from the 3-D thermal results or be obtained from the thermal analysis result using a consistent simplified model.

Finally, it is noted that the stress intensity can be closely related to the ΔΔT values, even in a three-dimensional situation. This correlation is useful in a preliminary design stage.

Although specific tube dimension, thermal load and material are considered in this investigation, it is believed that the main conclusion reached herein should also be helpful in a general situation of heat transfer tubes subject to axial temperature fluctuation.

TABLE 1 A Summary of Thermal and Elastic Stress Results of Various Rivulet Models

Thermal Model	Stress Model and Computer Code	Temperature, °C			Stresses, MPa			$S_{all}/\Delta\Delta T$, MPa/°C	$S_{eq}/\Delta\Delta T$, MPa/°C	CPU, s
		$T_{T/C\ max.}$	$\Delta T_{T/C}$	$\Delta\Delta T$	S_{all}	S_{mean}	S_{eq}			
I. 3-D (r, θ, z)										
A. 3-Rivulet	i. 3-D (r, θ, z), FEM	406.6	17.1	102.1	59.73	114.78	79.18	1.41	1.69	6691.1
	ii. 2-D (r, θ), FEM	"	"	"	60.53	114.31	80.13	1.46	1.91	7.8
	iii. 2-D (r, z), FEM	"	"	"	53.63	142.88	77.61	1.21	1.81	37.4
	iv. 2-D (r, z), FW-1059	"	"	"	53.09	139.77	76.12	1.26	1.81	1.2
	v. 1-D (r), FEM	"	"	"	50.57	141.89	72.99	1.20	1.71	1.7
	vi. 1-D (r), FW-1045	"	"	"	51.27	141.43	71.76	1.22	1.77	0.4
B. 4-Rivulet	i. 3-D (r, θ, z), FEM	403.3	12.0	38.4	51.97	115.44	69.28	1.35	1.81	7926
II. 2-D (r, θ)										
A. 3-Rivulet	i. 2-D (r, θ), FEM	408.2	17.5	43.2	62.13	115.82	82.92	1.44	1.92	2.0
	ii. 2-D (r, θ), FW-NONAX	"	"	"	63.02	117.26	84.46	1.46	1.95	0.9
B. 4-Rivulet	i. 2-D (r, θ), FEM	405.1	12.2	39.5	54.21	116.28	72.44	1.37	1.83	7.8
	ii. 2-D (r, θ), FW-NONAX	"	"	"	55.20	117.51	74.04	1.40	1.87	0.9

References

[1] CHIANG, T., FRANCE, D. M., and BUMP, T. K., "DNB Induced Thermal Stress and Fatigue in LMFBR Evaporator Tubes with Oxide Scale", ANL-CT-75-24, December 1974.

[2] CHU, C. L., WOLF, S., and DALCHER, A. W., "Oscillatory Dryout Related Thermal Stresses in Clean Steam Generator Tubes", ASME Paper No. 76-JPGC-NE-2, September 1976.

[3] FRANCE, D. M., CARLSON, R. D., CHIANG, T., and PRIEMER, R., "CHF-Induced Thermal Oscillations Measured in an LMFBR Steam Generator Tube Wall", ANL-CT-78-1, October 1977.

[4] CHU, C. L., ROBERTS, J. M., and DALCHER, A. W., "DNB Oscillatory Temperature and Thermal Stress Responses for Evaporator Tubes Based on Rivulet Model", ASME Paper No. 77-WA/NE-5, 1977.

[5] MAGEE, P. M., CASEY, D. F., CHU, C. L., DILLMAN, C. W., ROBERTS, J. M., and WOLF, S., "An Evaluation of Strain Cycling Effects in the DNB Zone of the CRBR Evaporators", GE Report NEDM-14164, Fast Breeder Reactor Department, General Electric Company, December 1976.

[6] KAO, T. T., KAMAL, S. A., PAI, D. H., CHERN, J. M., and CHO, S. M., "Combined Thermal and Stress Program for DNB Analysis of LMFBR Steam Generators", FWC/FWEC/ND-78-14, Foster Wheeler Energy Corporation, April 1978.

[7] MANSON, S. S., Thermal Stresses and Low-Cycle Fatigue, McGraw-Hill Book Company, 1966.

[8] ASME Boiler and Pressure Vessel Code, 1977 Edition, Section III, Paragraph NB-3216.

[9] ANSYS Engineering Analysis Systems, Swanson Analysis Systems, Incorporated, Pennsylvania, 1975.

[10] RAO, M. S., "NONAX - A Computer Program for Thermoelastic-Plastic-Creep Analysis of Thick Walled Cylinders Under General Nonaxisymmetric Loading", FWC/FWDC/EST-78-5, Foster Wheeler Development Corporation, November 1978.

[11] CHERN, J. M., and PAI, D. H., "Inelastic Behavior of Finite Circular Cylindrical Shells", ASME Journal of Pressure Vessel Technology, Vol. 99, February 1977, pp. 31 - 38.

[12] CHERN, J. M., and PAI, D. H., "A Simplified Tool for the Elevated Temperature Cyclic Analysis of Pressure Components", Second International Conference on Pressure Vessel and Piping Technology, Part I: Design and Analysis, San Antonio, Texas, 1973, pp. 263 - 275.

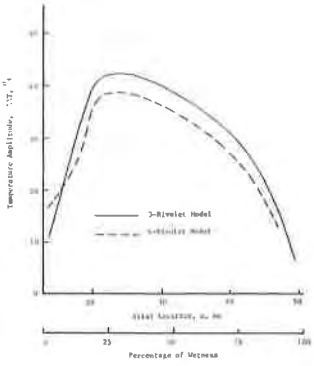

Fig. 1

Axial Distributions of Fluctuation Amplitudes of Temperature Different Through Tube Wall in Three-Dimensional Models

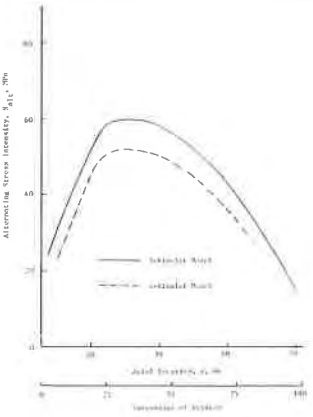

Fig. 2

Axial Distributions of Alternating Stress Intensity in Three-Dimensional Models

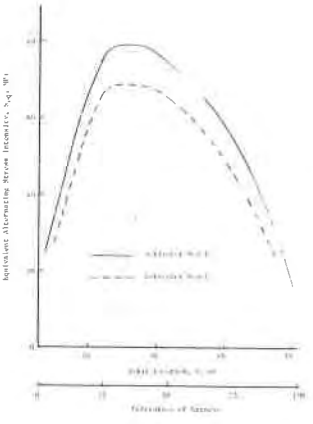

Fig. 3

Axial Distributions of Equivalent Alternating Stress Intensity in Three-Dimensional Models